Protein Science (1994), *3*:2217–2225. Cambridge University Press. Printed in the USA.

Contributions of a hydrogen bond/salt bridge network to the stability of secondary and tertiary structure in λ repressor

SUSAN MARQUSEE AND ROBERT T. SAUER

Department of Biology, Massachusetts Institute of Technology, Cambridge, Massachusetts 02139

(RECEIVED June 23, 1994; ACCEPTED September 13, 1994)

Abstract

In the N-terminal domain of λ repressor, the Asp 14 side chain forms an intrahelical, hydrogen bond/salt bridge with the Arg 17 side chain and a tertiary hydrogen bond with the Ser 77 side chain. By measuring the stabilities to urea denaturation of the wild-type N-terminal domain and variants containing single, double, and triple alanine substitutions at positions 14, 17, and 77, the side-chain interaction energies, the coupling energy between interactions, and the intrinsic effects of each wild-type side chain on protein stability have been estimated. These studies indicate that the Asp 14–Arg 17 and Asp 14–Ser 77 interactions are stabilizing by roughly 0.8 and 1.5 kcal/mol, respectively, but that Asp 14, by itself, is destabilizing by roughly 0.9 kcal/mol. We also show that a peptide model of α-helix 1, which contains Asp 14 and Arg 17, forms a reasonably stable, monomeric helix in solution and responds to alanine mutations at positions 14 and 17 in the fashion expected from the intact protein studies. These studies suggest that it is possible to view the stability effects of mutations in intact proteins in a hierarchical fashion, with the stability of units of secondary structure being distinguishable from the stability of tertiary structure.

Keywords: α-helix; interaction energy; mutants; peptide model; protein stability

Protein structure is generally described in a hierarchical fashion, distinguishing secondary from tertiary structure, and it would be useful if similar distinctions could be made at the level of protein stability. Do some residues serve to stabilize a protein by stabilizing a unit of secondary structure? Are other residues important solely for their effects on tertiary packing? If residues are involved in both secondary and tertiary interactions, is it possible to separate these effects? To address these questions, we sought to study the effects of destabilizing mutations in an α-helix of a protein and also in an isolated peptide model of the same α-helix.

In the work described here, we show that residues 9–23 of the N-terminal domain of λ repressor, which form α-helix 1 in the protein (Pabo & Lewis, 1982; Jordan & Pabo, 1988), also form a reasonably stable α-helix as an isolated peptide in aqueous solution. We also evaluate the contributions to repressor stability of 3 interacting residues: Asp 14 and Arg 17 in helix 1, and Ser 77 in the loop between helices 4 and 5 (Fig. 1; Kinemage 1). Each of these residues shows a highly restricted substitution pattern in genetic studies, suggesting that they play key roles in structure and/or function (Reidhaar-Olson & Sauer, 1990). In the crystal structure of the N-terminal domain (Pabo & Lewis, 1982; Jordan & Pabo, 1988), the Oδ1 atom of the Asp 14 side chain makes an intrahelical, hydrogen bond/salt bridge with the NH1 atom of the Arg 17 side chain and the Oδ2 atom makes a tertiary hydrogen bond with the Oγ of the Ser 77 side chain (Fig. 1; Kinemage 1). Most of the surface area (97%) of Asp 14 is inaccessible to solvent (Kinemage 2). The majority of this solvent exclusion arises from either local packing within the helix (53%) or interactions with the side chain of Ser 77 (27%). Ser 77 is completely inaccessible and Arg 17 is 60% inaccessible to solvent. To investigate the importance of residues 14, 17, 77, and their interactions, we constructed, purified, and characterized the 7 possible mutant proteins containing single, double, and triple alanine substitutions at these positions. The free energy of unfolding for each variant was measured by urea denaturation. Comparison of the relative stabilities for the different variant proteins allows an estimation of the side-chain interaction energies, the cooperative coupling of interactions, and the intrinsic effects of the substitutions. By constructing and determining the effects of the same alanine substitutions in the peptide model of helix 1, the intrinsic effects of the substitutions on helix formation have also been determined, allowing secondary and tertiary effects to be compared.

Reprint requests to Susan Marqusee at her present address: Division of Biochemistry and Molecular Biology, MCB: 229 Stanley Hall, University of California, Berkeley, California 94720; e-mail: susan_marqusee@maillink.berkeley.edu.

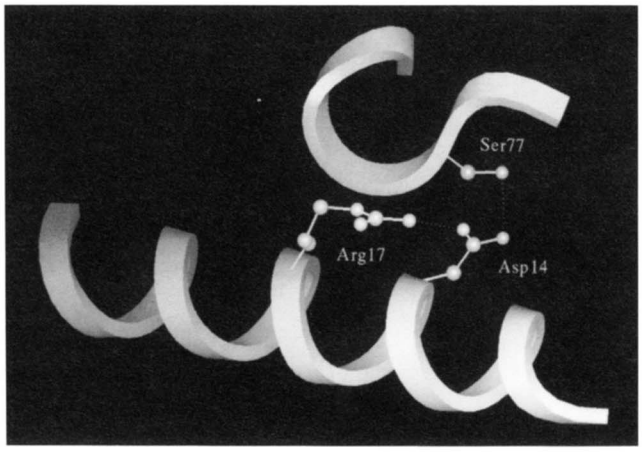

Fig. 1. Model of the hydrogen bond/salt bridge network between Arg 17, Asp 14, and Ser 77. Each of the hydrogen bonds is 2.8 Å. Coordinates taken from Jordan and Pabo (1988).

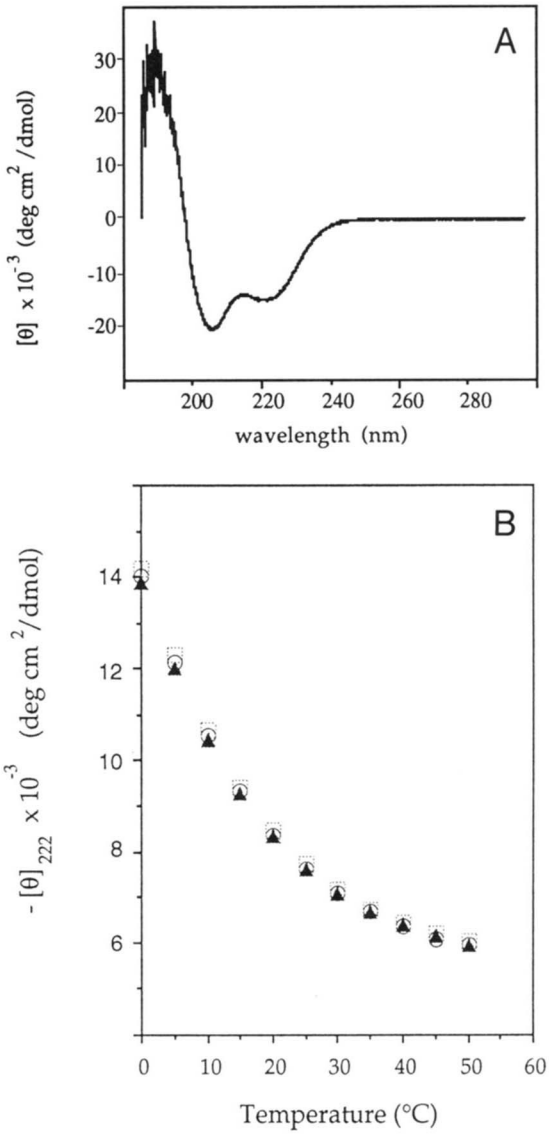

Fig. 2. A: CD spectrum for the wild-type peptide (λR1) in 0.1 M potassium fluoride (pH 7, 1 °C). **B:** Thermal unfolding of the peptide λR1 at several concentrations as measured by $-[\theta]_{222}$, the mean residue ellipticity at 222 nm (0.1 M KCl, pH 7.0). 24 μM peptide (○), 46 μM peptide (▲), and 89 μM peptide (□).

Results

Helix formation by a peptide consisting of residues 9–23

A peptide (λR1) corresponding to helix 1 (residues 9–23) of wild-type λ repressor was synthesized with its N- and C-termini blocked by acetylation and amidation, respectively (Kinemage 3). These blocking groups remove the formal charges at the ends of the peptide, which have the potential to destabilize a helix by interacting with the helix macrodipole (Scholtz & Baldwin, 1992). The blocking groups also provide a better model for the sequence in the context of the intact protein. Figure 2A shows that the far-UV CD spectrum of the λR1 peptide is characteristic of an α-helix with minima at 222 nm and near 208 nm. If we assume a mean-residue ellipticity at 222 nm ($[\theta]_{222}$) of −34,000 deg · cm^2/dmol for 100% helicity (Marqusee et al., 1989) and a value of 0 deg·cm^2/dmol for the random coil, then the λR1 peptide is ~40% helical under the conditions of the experiment (pH 7, 1 °C, 0.1 M KCl).

The helicity of λR1 decreases with increasing temperature as seen in Figure 2B. This temperature-induced denaturation is independent of peptide concentration over the range studied (10–100 μM), as would be expected if the λR1 peptide is monomeric in solution.

^{1}H-NMR spectroscopy also demonstrates that the wild-type peptide λR1 exists in a partially helical conformation. A summary of 2-dimensional NOE data is shown in Figure 3. $d_{NN}(i, i+1)$ connectivities were observed throughout the entire peptide. Similarly, $d_{\alpha N}(i, i+3)$ and $d_{\alpha\beta}(i, i+3)$ connectivities were observed in all portions of the peptide. These connectivities are indicative of helix formation and suggest that each residue in the peptide spends a significant fraction of time in a helical conformation.

Mutant peptide analogues

To determine the roles of the Asp 14 and Arg 17 side chains in stabilizing helix formation, we synthesized peptide variants containing the Arg 17 → Ala mutation (λR2), the Asp 14 → Ala mutation (λR3), and the double mutation (λR5). Table 1 lists the extent of helix formation as measured by CD for all 4 peptides at 1 °C, pH 7. Replacing Arg 17 with Ala (λR2) reduces helix formation: $-[\theta]_{222}$ decreases from 14,000 to 6,500 deg·cm^2/dmol. Replacing Asp 14 with Ala (λR3), however, increases helix formation: $-[\theta]_{222}$ increases to 21,000 deg·cm^2/dmol. The double mutant (λR5) shows approximately the same amount of helicity as the wild-type peptide. At first glance, the mutant peptide data would seem to suggest that the Asp 14–Arg 17 salt bridge does not stabilize the isolated peptide, because breaking this interaction by the Asp 14 → Ala mutation (λR3) actually stabilizes the peptide helix. However, as we discuss below, it is possible that the salt bridge is helix-stabilizing but is more than offset by an intrinsic helix-destabilizing effect of Asp 14.

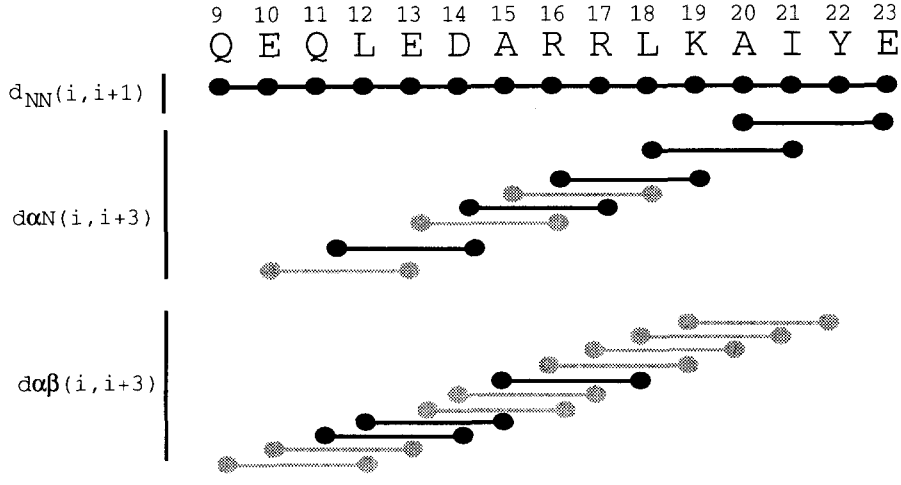

Fig. 3. Summary of 2D NOESY data on the λR1 peptide (4 °C). Dark bars indicate that NOESY crosspeaks could be assigned unambiguously to a unique pair of protons. Shaded lines indicate that the NOESY crosspeaks were observed but could not be assigned unambiguously.

Protein studies

Mutant variants of the N-terminal domain of λ repressor containing all possible combinations of single, double, and triple alanine substitutions at positions 14, 17, and 77 were constructed, purified, and named by the 1-letter code for the residue at each position. For example, DRS is wild type and DAS designates the protein containing Asp 14, Ala 17, and Ser 77. All 7 variants were able to fold and adopt a λ repressor-like structure as demonstrated by DNA-binding activity in vivo, CD spectra, and 1-dimensional NMR spectroscopy. The activity data in vivo are shown in Figure 4. Each of the protein variants exhibits some repressor activity, although this activity is temperature sensitive and no protein is as active as wild type. The CD spectrum for each of the protein variants was predominantly helical and indistinguishable from wild type.

In 1-dimensional ^{1}H-NMR studies, all of the proteins displayed similar chemical dispersion, indicating similar structures. The N-terminal domain of λ repressor contains 7 aromatic groups (5 tyrosines and 2 phenylalanines), whose proton resonances have been assigned (Weiss et al., 1987a). Three of the aromatic groups (Tyr 22, Phe 51, and Phe 76) are buried in the folded protein and their chemical shifts therefore provide probes of tertiary structure. As shown in Figure 5, the overall pattern of resonances in this region is similar in all of the proteins, although some variants show small changes in the chemical shifts of specific protons. The largest variation occurs in the resonances of the ring protons of Phe 76, which are shifted in variants containing the nearby Ser 77 → Ala mutation. Such shifts could reflect changes in magnetic environment caused by loss of the neighboring Ser 77–Asp 14 interaction or local structural changes.

Table 1. *Peptide sequences and helix-forming properties*

Peptide[a]	9	14	17	23	$[\theta]_{222}$ (cm^2 deg/dmol)	% Helix[b]
λR1	Ac-QEQLE**D**A**R**R**L**KAIYE-NH_2				−14,000	41
λR2	Ac-QEQLE**D**A**R**A**L**KAIYE-NH_2				−6,500	19
λR3	Ac-QEQLE**A**A**R**R**L**KAIYE-NH_2				−21,000	62
λR5	Ac-QEQLE**A**A**R**A**L**KAIYE-NH_2				−15,000	44

[a] The α-NH_2 is blocked by an acetyl group (Ac), and the α-COOH is blocked by an amide group (NH_2).

[b] % Helix calculated based on an estimate of $[\theta]_{222} = -34{,}000$ deg·cm^2/dmol for 100% helix and 0 for 0% helix.

Stability studies, interaction energies, and mutant cycles

Unfolding free energies were determined by monitoring CD ellipticity as a function of the concentration of urea at 25 °C. Figure 6 shows data for the denaturation of the DAS mutant. Values for ΔG_{H_2O} (the free energy of protein unfolding in the absence of urea) and C_m (the urea concentration at which half of the protein molecules are unfolded) are listed in Table 2.

Thermodynamic cycles can be used to assess the apparent energy of interaction between 2 residues and the cooperativity of interactions (Horovitz & Fersht, 1990; Horovitz et al., 1990).

Table 2. *Free energies of unfolding of protein variants of the N-terminal domain of λ repressor determined by urea denaturation*

Protein	ΔG_{H_2O}[a] (kcal/mol)	C_m[b] (M)	$\Delta\Delta G$[c] (kcal/mol)
DRS	4.82	4.42	–
ARS	3.65	3.34	−1.17
DAS	3.67	3.36	−1.15
DRA	3.46	3.17	−1.36
AAS	3.32	3.05	−1.50
ARA	3.82	3.50	−1.00
DAA	2.55	2.34	−2.27
AAA	3.43	3.15	−1.39

[a] Free energy of unfolding in the absence of urea at 25 °C, 0.1 M KCl, pH 7, calculated as $m * C_m$ with $m = 1.09$ kcal/mol-M (see Materials and methods).

[b] Urea concentration at the midpoint of the transition.

[c] Change in stability from wild type.

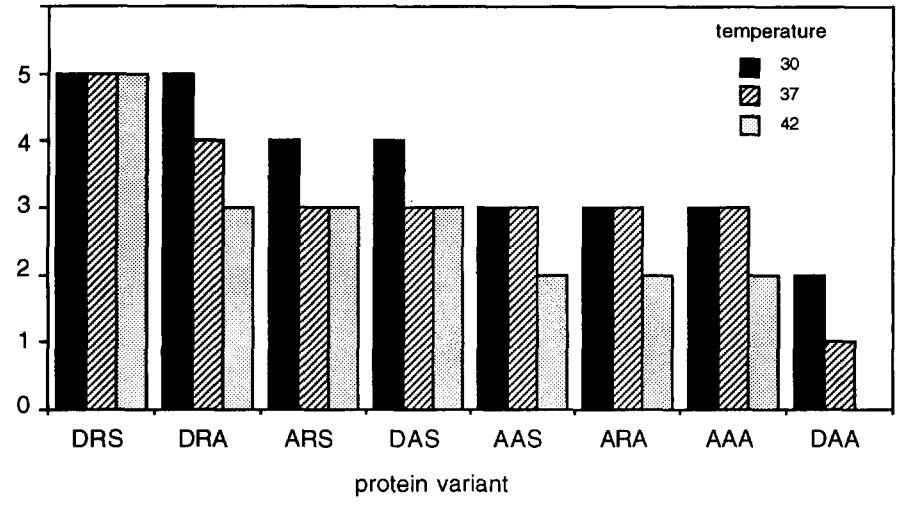

Fig. 4. Activity profiles in vivo for 14/17/77 protein variants as monitored by the immunity of cells to virulent phage infection at 30, 37, and 42 °C. Vertical bar height indicates level of phage resistance (0 = KH54 sensitive; 1 = λ clc17 sensitive/KH54 resistant; 2 = λ vir sensitive/clc17 resistant; 3 = λ 3v sensitive/λ vir resistant; 4 = λ 4v sensitive/λ 3v resistant; 5 = λ 5v sensitive/λ 4v resistant).

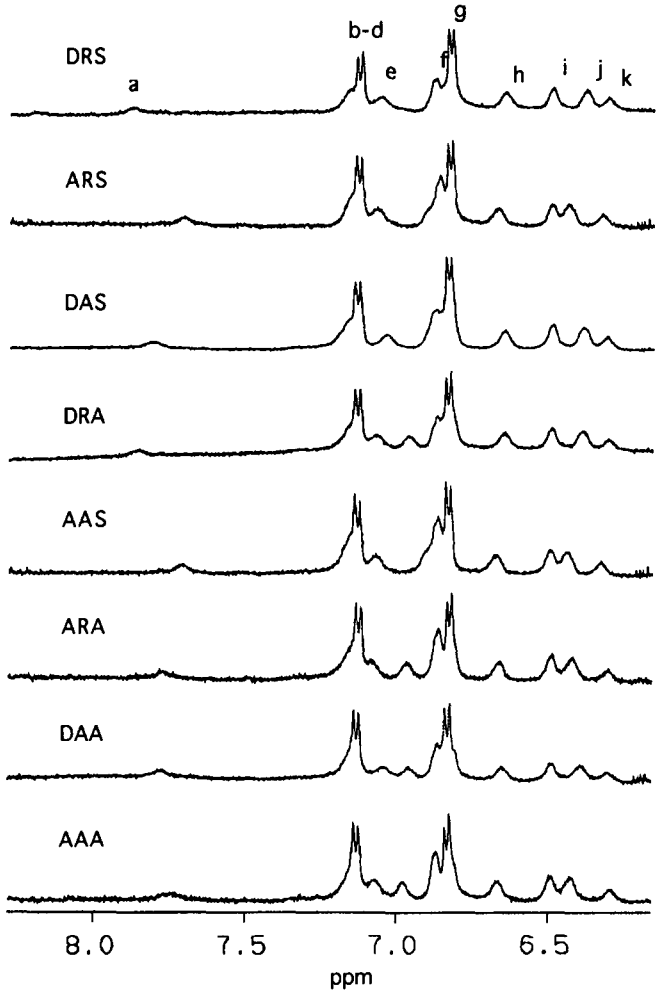

Fig. 5. Aromatic ^{1}H-NMR spectra of wild type (DRS) and the 7 mutant proteins in D_2O (25 °C). The wild-type resonances (Weiss et al., 1987a) are labeled a–k (a: Phe 76 para; b: Tyr 85 ortho; c: Tyr 60 ortho; d: Tyr 101 ortho; e: Phe 76 meta; f: Phe 76 ortho, Tyr 60 meta; g: Tyr 85 meta, Tyr 101 meta, Phe 51 ortho; h: Tyr 22 ortho; i: Tyr 22 meta, Tyr 88 ortho; j: Phe 51 meta; k: Phe 51 para).

Mutating a single residue involved in an interaction may simultaneously alter a number of factors within the protein. A double mutant cycle, however, evaluates a site substitution both in the presence and absence of the interacting side chain. The apparent energy of interaction between 2 side chains (ΔG_{int}) can be calculated as the difference in the free energy of unfolding upon mutating one of the partners in the presence or absence of the other partner. This is equal to the difference between opposing $\Delta\Delta G$'s, for example between the 2 vertical or 2 horizontal terms, in thermodynamic cycles like those shown in Figure 7. Formally, ΔG_{int} includes energetic terms for the hydrogen bonding and electrostatic interactions between the wild-type residues, terms for packing and hydrophobic interactions between the side chains, terms for changes in desolvation that depend upon in-

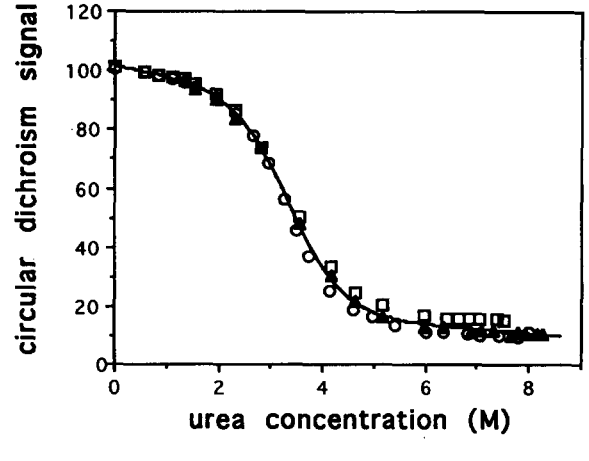

Fig. 6. Urea denaturation of the DAS mutant as measured by CD (25 °C, 0.1 M KCl, 50 mM potassium phosphate, pH 7.1). Different symbols represent data from 3 independent experiments. The line shows the theoretical curve for $\Delta G_{H_2O} = -3.67$ kcal/mol and $m = 1.09$ kcal/mol-M, calculated as described in the Materials and methods. An independent nonlinear least-squares fitting of the 3 combined data sets gave $\Delta G_{H_2O} = -3.65$ kcal/mol and $m = 1.10$ kcal/mol-M. The square roots of the variance of the 2 fits were 2.05 and 2.07, respectively.

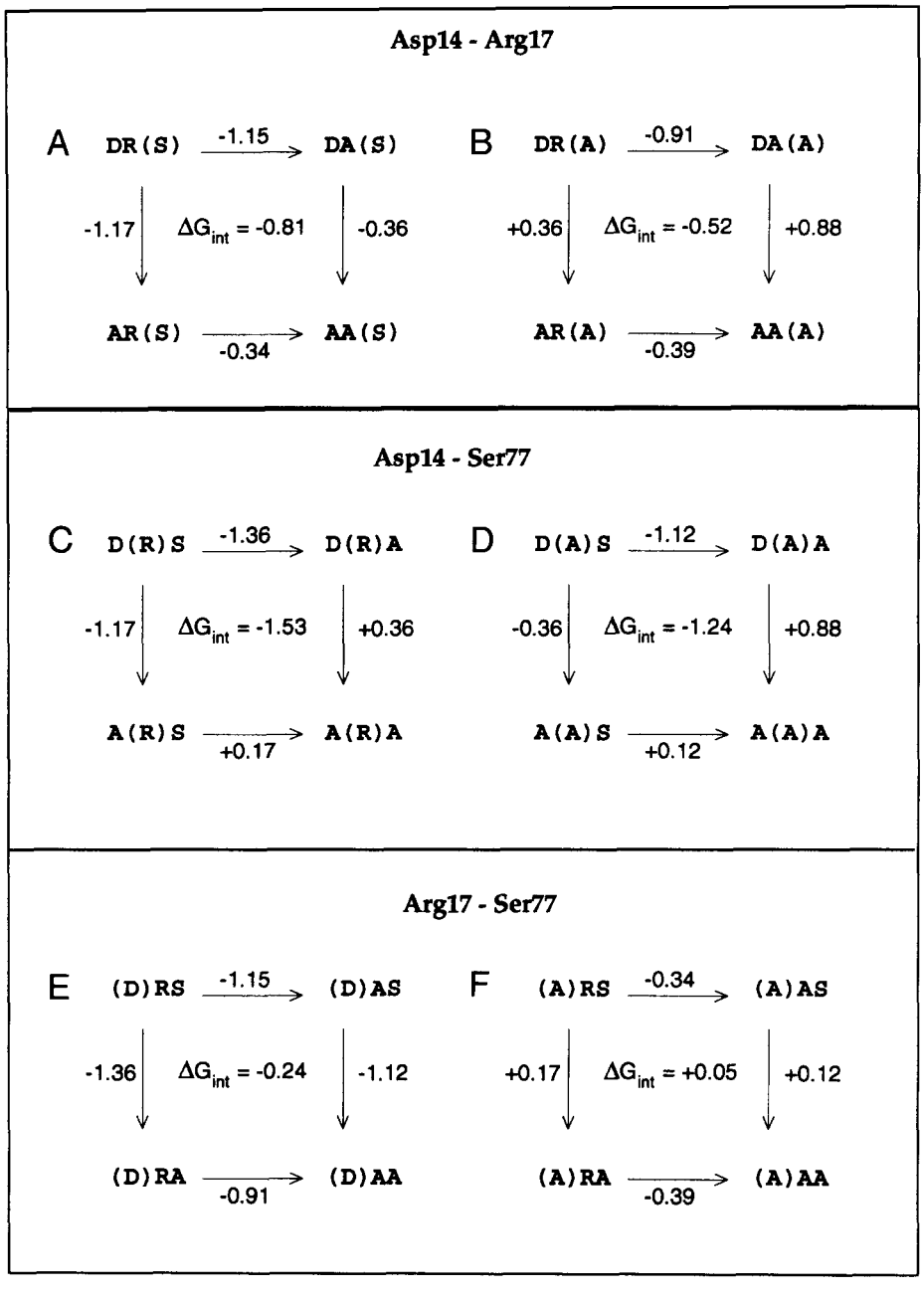

Fig. 7. Double mutant cycles representing all 6 faces of the triple mutant cube. The invariant residue in each cycle is in parentheses. The free energy changes for each mutation are calculated from the values in Table 2.

teractions between the wild-type and mutant side chains, and terms for any structural relaxation in the native and/or denatured states that depends upon side-chain interactions.

Asp 14–Arg 17 interaction

A mutant cycle for the interaction between Asp 14 and Arg 17 in the background of the wild-type serine at position 77 can be constructed from the stabilities of the 4 proteins DRS, DAS, ARS, and AAS (Fig. 7A; Kinemage 2). The wild-type protein, DRS, is the most stable: the urea concentration at the midpoint of the transition, C_m, is 4.42 M. Single site substitutions, which disrupt the Asp 14–Arg 17 salt bridge, destabilize the protein: C_m = 3.34 M for ARS and 3.36 M for DAS. The double mutant AAS is the least stable with a C_m of 3.05 M. The effects of these mutations upon stability are not additive as can be seen by the −0.81 kcal/mol difference between the vertical or horizontal $\Delta\Delta G$'s in the cycle for Figure 7A. This negative value of ΔG_{int} suggests that the wild-type Asp 14 and Arg 17 side chains interact favorably to stabilize the protein.

The unfolding studies reported above were performed in a buffer containing 0.1 M KCl. To determine the salt sensitivity of the Asp 14–Arg 17 interaction, unfolding studies were also repeated in high salt (Table 3). The apparent interaction energy

Table 3. *Free energies of unfolding at 1.0 M KCl for the 14/17 variants as determined by urea denaturation*

	ΔG_{H_2O}[a] (kcal/mol)	C_m[b] (M)	$\Delta\Delta G$[c] (kcal/mol)
DRS	5.91	5.69	–
ARS	4.73	4.55	−1.18
DAS	4.97	4.78	−0.94
AAS	4.42	4.25	−1.49

[a] Free energy of unfolding in the absence of urea at 25 °C, 1 M KCl, pH 7, calculated as $m * C_m$ with m = 1.04 kcal/mol-M.
[b] Urea concentration at the midpoint of the transition.
[c] Change in stability from wild type.

in 1.0 M KCl (25 °C) is −0.52 kcal/mol. Although this is a smaller value than that obtained in 0.1 M KCl, it is substantial enough to indicate that the Asp 14–Arg 17 interaction is not effectively screened by salt.

Asp 14–Ser 77 interaction

A mutant cycle for the Asp 14–Ser 77 interaction can be constructed from the stabilities of the 4 proteins DRS, ARS, DRA, and ARA (Fig. 7C). Once again, the wild-type protein DRS is the most stable (C_m = 4.42 M). The single-site changes are least stable with C_m's of 3.34 M (ARS) and 3.17 M (DRA). The double mutant, ARA, is less stable than wild type but more stable than the single mutants, with C_m = 3.50 M. ΔG_{int} for the Asp 14–Ser 77 interaction calculated from these data is −1.53 kcal/mol.

Coupling between the Asp 14–Arg 17 and the Asp 14–Ser 77 interactions

To what extent does the Asp 14–Arg 17 interaction help stabilize the Asp 14–Ser 77 interaction and vice versa? The coupling or interdependence of the 2 interactions in the triad can be calculated as the difference in the ΔG_{int}'s determined for the Asp 14–Arg 17 interaction in the presence or in the absence of Ser 77 or, alternatively, as the difference in the ΔG_{int}'s for the Asp 14–Ser 77 interaction in the presence or absence of Arg 17. The stabilities of the 4 mutant proteins DRA, ARA, DAA, and AAA comprise a mutant cycle for analyzing the Asp 14–Arg 17 interaction in the presence of the Ser 77 → Ala substitution (Fig. 7B). ΔG_{int} for the Asp 14–Arg 17 interaction in the presence of Ala 77 is −0.52 kcal/mol. Comparing this with the interaction energy of −0.81 kcal/mol determined in the presence of Ser 77 (Fig. 7A) yields a coupling energy between these 2 interactions of −0.29 kcal/mol. As required by thermodynamic linkage, the same coupling energy is found when examining the Asp 14–Ser 77 interaction in the presence of arginine or alanine at position 17 (Fig. 7C,D).

Intrinsic effects of Asp 14, Arg 17, and Ser 77

The intrinsic effects of each side chain on protein stability can be measured in the absence of the interacting side chains. For example, by comparing the mutants DAA and AAA (Table 2; Fig. 7), it can be seen that Asp 14 is intrinsically destabilizing. In the absence of the stabilizing interactions with Ser 77 and Arg 17, the change of Asp 14 → Ala *increases* protein stability by 0.88 kcal/mol. This is similar in magnitude to the stabilizing energy observed for the Asp 14–Arg 17 interaction. The interactions with Ser 77 and Arg 17 compensate for this intrinsic destabilizing effect of Asp 14 and account for its apparent stabilizing effect in the presence of the other residues. In the absence of other interactions, Ser 77 destabilizes the protein by 0.12 kcal/mol relative to alanine (AAS → AAA) and Arg 17 stabilizes the protein by 0.39 kcal/mol relative to alanine (ARA → AAA).

Discussion

To probe the importance of 3 interacting side chains (Asp 14, Arg 17, and Ser 77) in determining the thermodynamic stability of the N-terminal domain of λ repressor, changes in protein stability resulting from single, double, and triple alanine substitutions have been measured. In addition, to evaluate the role of Asp 14 and Arg 17 in stabilizing the α-helix in which they reside, helix formation was measured for peptide models containing the wild-type sequence and alanine-substituted variants. In the discussion that follows, we consider and interpret the results of these experiments with respect to several questions. These include: To what extent do the hydrogen bonding and salt-bridge interactions seen in the wild-type crystal structure contribute to protein stability? Does physical coupling of interactions result in strong energetic coupling? Is it reasonable to distinguish secondary from tertiary interactions in discussing and thinking about protein stability?

The Asp 14–Arg 17 hydrogen bond/salt bridge

The hydrogen bond/salt bridge between Asp 14 and Arg 17 involves side chains at the i and $i + 3$ positions of α-helix 1 in λ repressor. By thermodynamic cycle analysis, ΔG_{int} for the 14–17 interaction is favorable by roughly ~0.8 kcal/mol in 0.1 M KCl and by ~0.5 kcal/mol in 1.0 M KCl. It is not formally possible to equate these observed "interaction" energies with the strength of the hydrogen bond/salt bridge because factors including other interactions between the Asp 14 and Arg 17 side chains, and relaxation of the structures of the native and denatured states may also contribute. Nevertheless, the net effect of all of these factors is still a favorable contribution to protein stability. Moreover, it seems likely that the hydrogen bond/salt bridge does make a substantial contribution because the available data suggest that the mutant and wild-type proteins have similar global folds and any structural relaxation in the native protein should act to dampen the detrimental effects of the mutations, and thus lead to an underestimate of the importance of the wild-type interaction.

The importance of salt-bridge interactions in stabilizing proteins varies and appears to be highly dependent upon factors such as the screening of the charges by solvent, the cost of desolvating the charged groups to form the salt bridge, and the relative flexibility of the side chains involved in the ion pair (for review, see Yang & Honig, 1992). In general, solvent-exposed salt bridges seem to play little role in stabilizing proteins (Dao-Pin et al., 1991). In barnase, for example, a solvent-exposed intrahelical salt bridge between Asp 12 and Arg 16 has a negligible

interaction energy at salt concentrations above 0.1 M (Serrano et al., 1990). By contrast, salt bridges that are completely or partially solvent inaccessible generally appear to be more stabilizing. The λ repressor Asp 14–Arg 17 salt bridge, which is substantially buried, is similar in energy to the partially buried interaction found between the chain termini in bovine pancreatic trypsin inhibitor (~1 kcal/mol) (Brown et al., 1978). These interaction energies are modest, however, in comparison to those of buried ion pairs in T4 lysozyme and chymotrypsin, which are stabilizing by roughly 3–5 kcal/mol (Fersht, 1972; Anderson et al., 1990).

The Asp 14–Ser 77 hydrogen bond

The side chain of Asp 14 also forms a hydrogen bond with the side chain of Ser 77 (Fig. 1). ΔG_{int} for the 14–77 interaction is ~1.5 kcal/mol. With the caveats mentioned above, it seems likely that the hydrogen bond between these residues makes a substantial contribution to this interaction energy and plays a major factor in the low tolerance to substitution observed for Ser 77 (Reidhaar-Olson & Sauer, 1990). In T4 lysozyme, a hydrogen bond involving Thr 157 also appears to be quite important; single side-chain substitutions that disrupt this interaction destabilize the protein by ~1–2 kcal/mol (Alber et al., 1987). Hydrogen bonds formed between side chains and the amino and carboxy termini of helices have also been found to play important roles in stabilizing proteins (Serrano & Fersht, 1989).

Coupling between interactions

The cooperative nature of protein folding implies that many amino acid interactions must be energetically coupled. In the case of 3 interacting residues, one might expect that the first interaction helps to orient one of the side chains involved in the second interaction, thereby reducing the entropic cost and making the second interaction more favorable. Indeed, Barlow and Thorton (1983) have reported that 37% of ion pairs in protein crystal structures occur as charge networks, and for a triad of intrahelical salt bridges in barnase, the strength of either single salt bridge is decreased by more than 50% in the absence of the other interaction (Horovitz et al., 1990). The 14–17–77 interactions in λ repressor show some cooperative stabilization; the strengths of the 14–17 and 14–77 interactions are increased by ~0.3 kcal/mol in the presence of the other interaction. This coupling energy is modest, however, in comparison with the interaction energies.

Intrinsic destabilization of Asp 14

In the presence of Ala 17 and Ala 77, the Asp 14 → Ala mutation increases protein stability by 0.88 kcal/mol. This indicates that in the absence of the stabilizing side-chain interactions with Arg 17 and Ser 77, the side chain of Asp 14 *destabilizes* the folded protein. What causes this intrinsic destabilization? The $\chi 1$ angle for Asp 14 is roughly $-80°$ (g^+), the rotamer conformation most frequently observed for aspartic acid in α-helices (McGregor et al., 1987). However, this apparently favorable side-chain geometry places the Oδ1 side-chain oxygen of Asp 14 within 3.5 Å of the backbone carbonyl oxygens at position 76 and at position 10 ($i-3$) in helix 1. These interactions are electrostatically unfavorable and could account for some or all of the destabilizing effect of Asp 14, assuming that the $\chi 1$ angle remained the same in the absence of the Arg 17 and Ser 77 interactions. This assumption is reasonable given that the g^- and t side-chain rotamers would result in a set of unfavorable van der Waals contacts of less than 3 Å for Asp 14. If conformation of the Asp 14 side chain is constrained by local packing, even in the absence of the Arg 17 and Ser 77 interactions, then it is not surprising that the coupling energy for the 14–17 and 14–77 interactions is modest.

Aspartic acid is considered to be a helix-breaking residue (Sueki et al., 1984). The intrinsic destabilizing effect of Asp 14 relative to alanine in an α-helical context in λ repressor is generally similar to those reported for Asp → Ala changes in a model coiled-coil system (0.62 kcal/mol; O'Neil & DeGrado, 1990) and in an α-helix in barnase (~0.6 kcal/mol; Horovitz et al., 1990). In the isolated peptide model of λ repressor's helix 1, Asp 14 is also helix destabilizing. If the helix 1 peptide existed only in the all-helix ($\theta = -34{,}000$) or all-coil states ($\theta = 0$), then the Asp 14 → Ala substitution in the background of Ala 17 would stabilize the peptide helix by 0.7 kcal/mol. Unfortunately, helix–coil transitions for peptides are not 2-state because molecules with intermediate degrees of helicity are usually present. Nevertheless, if the mutant change affected the stability of the all-helical state and partially helical states to the same extent relative to the coil state, then the free energy value cited above would still be valid. Irrespective of the detailed energetics, however, it is clear that the intrinsic destabilizing effect of Asp 14 in the intact protein is also observed in the peptide model.

Peptide model of helix formation

The peptide analogue of λ repressor's helix 1 is about 40% α-helical in solution, making it one of a relatively small number of protein fragments that form reasonably stable helices in isolation. For example, in a recent report by Munoz and Serrano (1994), only 5 of 100 peptides corresponding to helical segments of proteins had helicities greater than 40%, and the vast majority contained less than 10% helix. At present, we do not know why the helix 1 peptide of λ repressor is so stable in solution. Intrahelical salt bridges have been demonstrated to be helix stabilizing in short peptides of de novo design (Marqusee & Baldwin, 1987). However, the Asp 14–Arg 17 salt bridge does not appear to be a significant factor in the stability of the peptide helix, presumably because most if not all of the stabilizing effects of the interaction are offset by the intrinsic destabilizing effect of Asp 14. Many of the residues in the λR1 peptide (Table 1) are good helix formers, and the amino acid composition of the peptide may simply favor helix formation. Alternatively, the stability of this peptide may result from some as yet undetermined sequence-specific interactions.

Comparison between the protein and peptide stability

How useful are peptide models in understanding the stability properties of intact proteins and vice versa? We find that a mutant cycle constructed from the isolated peptide data parallels that observed for the protein in the background of Ala at position 77. The mutation Arg 17 → Ala is destabilizing in both contexts, whereas the mutation Asp 14 → Ala is stabilizing in both contexts. In both cycles, the double alanine mutant (λR5 and AAA) is about equal to or slightly greater in stability than the

counterpart containing both Asp 14 and Arg 14 (λR1 and DRA). These data suggest that peptide studies do provide meaningful models for understanding native proteins, and also suggest that the energetic contributions to stability of residues like Asp 14 can be interpreted in a hierarchical fashion in which specific interactions can contribute to stabilization of secondary structure and/or tertiary structure.

Materials and methods

Mutagenesis

Mutants were constructed by ligating double-stranded mutagenic cassettes into plasmid backbone fragments from pWL104 or pWL103. Both plasmids encode residues 1–102 of λ repressor, contain numerous restriction sites in the 1–102 gene, and contain phage m13 origins of replication (Lim & Sauer, 1989). Plasmid pWL103 is identical to pWL104 except for an *Nco* I site at the N-terminus of the gene. The gene for the ARS protein was constructed by ligating a cassette between the *Bss* HII and *Sac* I sites in pWL104. The genes for the DAS and AAS proteins were obtained by ligating a cassette between the *Nco* I and *Bss* HII sites in pWL103. The gene for the DRA protein was available from a previous study (Reidhaar-Olson & Sauer, 1990). Genes encoding the ARA, DAA, and AAA proteins were constructed by combining the appropriate restriction fragments from the genes encoding the DAS, AAS, DRA, and ARS proteins.

Mutant plasmids were transformed into *Escherichia coli* strain X90, and single-stranded plasmid DNA was prepared by infecting cells with the helper phage RV1. The sequence of each of the mutant genes was confirmed by DNA sequencing using the dideoxynucleotide method and the T7 sequenase system (US Biochemical). Cells harboring mutant proteins were assayed for repressor activity by cross-streaking a fresh colony against clear or virulent derivatives of phage λ as described (Lim & Sauer, 1991).

Protein purification

The purified N-terminal domain (residues 1–102) of wild-type λ repressor was obtained as a gift from John Reidhaar-Olson. Mutant variants of the N-terminal domain were expressed in *E. coli* strain X90 or in strain DP748, a dnaJ$^-$ strain that allows higher-level expression of some unstable variants (Reidhaar-Olson et al., 1990). Mutant proteins were purified as described (Lim & Sauer, 1991) using column chromatography on Affigel Blue, Biorex 70, and Sephadex G-75. Purified proteins were judged to be >95% homogeneous following SDS polyacrylamide gel electrophoresis and staining with Coomassie blue. Proteins were stored frozen at −20 °C in a buffer containing 10 mM Tris HCl, pH 8, 2 mM $CaCl_2$, 0.1 M EDTA, 5% (v/v) glycerol, and 50 mM KCl. Aliquots were thawed, dialyzed extensively into CD buffer (0.1 M potassium chloride, 50 mM potassium phosphate, pH 7.0), and stored at 4 °C until needed. No difference in CD signal was observed over months of storage at 4 °C.

Peptide synthesis and purification

All peptides except λR1 were synthesized by solid-phase peptide synthesis on a Milligen 9050 peptide synthesizer using 9-fluorenyl methoxycarbonyl (FMOC) chemistry (Stewart & Young, 1984). λR1 was synthesized on an Applied Biosystem 431 peptide synthesizer using *N*-tert-butyloxycarbonyl (t-BOC) chemistry. Peptides were synthesized as C-terminal amides by using a *p*-methylbenzhydralamine resin. The α-NH_2 group of each peptide was acetylated with acetic anhydride. Following synthesis, peptides were desalted on Sephadex G-25 in 10 mM HCl and then purified by reverse-phase chromatography (C4 or C18) using a gradient of 10–60% acetonitrile in 0.1% trifluoroacetic acid. The identity of the purified peptides was confirmed by fast atom bombardment mass spectrometry.

CD measurements

CD measurements were made using an Aviv 60DS spectropolarimeter equipped with a Hewlett Packard 89100A temperature-controlled sample holder and a 10-mm-pathlength cuvette. Peptide samples were prepared by dilution from an aqueous stock (~2 mM peptide) into CD buffer. The concentration of peptide stock solutions was determined by measuring the absorbance at 275 nm of the single tyrosine in 6 M GuHCl and using an extinction coefficient of 1,450 cm^{-1} (Brandts & Kaplan, 1973). All CD experiments with peptides were performed using ~20 μM samples unless noted.

Protein unfolding reactions were assayed by monitoring the CD ellipticity at 222 nm or 225 nm as a function of urea concentration. Experiments were performed at 25 °C using protein samples at a concentration of ~35 μg/mL (3 μM). Because the N-terminal domain of λ repressor forms only a weak dimer (K_d = 300 μM; Weiss et al., 1987b), the protein is predominantly monomeric (~98%) at this concentration. For denaturation studies, protein samples were prepared with and without 9 M urea. Except for the urea, both samples were identical in containing the same concentration of protein and a buffer consisting of 50 mM potassium phosphate (pH 7) and 100 mM potassium chloride. Samples containing intermediate concentrations of urea were prepared by mixing the appropriate amounts of the high denaturant and no denaturant samples. Samples were equilibrated at least 5 min at every urea concentration and the CD signal at 222 or 225 nm was averaged for 2 min. No change in CD signal was observed when the incubation time was varied from a few seconds to hours, indicating that equilibrium is reached rapidly. Similar curves of CD signal versus denaturant were also obtained from experiments performed in the folding and unfolding directions, again suggesting that the reaction is at equilibrium and is fully reversible.

Analysis of chemical denaturation and free energy determination

The free energy of unfolding was determined assuming a 2-state model (N ⇌ D) and a linear dependence of free energy on denaturant concentration (Pace, 1986):

$$\Delta G_u = \Delta G_{H_2O} - m * [\text{urea}]$$

$$= -RT \ln K_u = -RT \ln \left[\frac{y_N - y}{y - y_D} \right],$$

where ΔG_{H_2O} is the extrapolated free energy in the absence of denaturant, y is the observed CD signal, and y_N and y_D are the

ellipticities characteristic of the native and denatured states. The constant m measures the dependence of ΔG_u on denaturant concentration. Multiple data sets were collected for the denaturation of each protein and fit using the program NONLIN (Santoro & Bolen, 1988) to the equation

$$y = \frac{(y_f + m_f * [\text{urea}]) + (y_u + m_u * [\text{urea}]) * (\exp[-\Delta G_u/RT])}{1 + \exp[-\Delta G_u/RT]}$$

In this equation, ΔG_u is a function of ΔG_{H_2O}, m, and urea as described above, and y_f, m_f and y_u, m_u are the zero-denaturant intercepts and slopes for the native and denatured baselines respectively. When all 6 parameters (ΔG_{H_2O}, m, y_f, m_f, y_u, and m_u) were allowed to vary in the fitting procedure, the reproducibility of the C_m values (calculated as $\Delta G_{H_2O}/m$) determined for independent melts of the same protein was very good, but the reproducibility of the ΔG_{H_2O} values was relatively poor. To improve reproducibility, the data were refit allowing only ΔG_{H_2O}, y_f, and y_u to vary and using average values determined for m, m_f, and m_u from the 6 parameter fits. The average m value for all of the variants was 1.09 (±0.05) kcal/mol-M. This procedure gave good reproducibility (±1.5%) for ΔG_{H_2O} from independent melts and also gave good overall statistics for the fit (see legend to Fig. 6).

^{1}H-NMR spectroscopy

NMR spectra were taken on a Bruker AM 500 spectrometer. Chemical shifts are referenced to 3-(trimethylsilyl)-1-propanesulfonic acid (TSP) at 0.0 ppm. Proteins were dialyzed against 50 mM ammonium bicarbonate, lyophilized, resuspended in 99% pure D_2O, and lyophilized to dryness. Samples at protein concentrations of ~100 μM were resuspended in a deuterium buffer of 50 mM potassium phosphate, 0.1 M KCl (pD 7.1, uncorrected). One-dimensional spectra, taken at 17 °C, are the sum of 2,048 scans and were processed with a 3-Hz line-broadening function. Samples of the wild-type peptide (λR1) were prepared by dissolving dry peptide in a 90:10% H_2O:D_2O per-deuterated acetate buffer (pH 4.5, room temperature) to a concentration of ~5 mM. Double quantum-filtered correlation spectroscopy, total correlation spectroscopy, and NOE spectroscopy spectra were recorded, and resonances were assigned by sequential assignment methods (Wüthrich, 1986).

Acknowledgments

This work was supported by NIH grant AI-15706 and by a Helen Hay Whitney postdoctoral fellowship (S.M.). We thank Rheba Rutkowski for assistance in peptide synthesis, Lawrence McIntosh for help with the NMR studies, and members of the Sauer laboratory for helpful advice and discussions.

References

Alber T, Sun DP, Wilson K, Wozniak JA, Cook SP, Matthews BW. 1987. Contributions of hydrogen bonds of Thr 157 to the thermodynamic stability of phage T4 lysozyme. *Nature 330*:41–46.

Anderson DE, Becktel WJ, Dahlquist FW. 1990. pH-induced denaturation of proteins: A single salt bridge contributes 3–5 kcal/mol to the free energy of folding of T4 lysozyme. *Biochemistry 29*:2403–2408.

Barlow DJ, Thornton JM. 1983. Ion-pairs in proteins. *J Mol Biol 168*: 867–885.

Brandts JF, Kaplan LJ. 1973. Derivative spectroscopy applied to tyrosyl chromophores. Studies on ribonuclease, lima bean inhibitors, insulin and pancreatic trypsin inhibitor. *Biochemistry 12*:2011–2024.

Brown LR, Demarco A, Richarz R, Wagner G, Wüthrich K. 1978. The influence of a single salt bridge on static and dynamic features of the globular solution conformation of the basic pancreatic trypsin inhibitor. *Eur J Biochem 88*:87–95.

Dao-Pin S, Sauer U, Nicholson H, Matthews BW. 1991. Contributions of engineered surface salt bridges to the stability of T4 lysozyme determined by directed mutagenesis. *Biochemistry 30*:7142–7153.

Fersht AR. 1972. Conformational equilibria in α- and δ-chymotrypsin. *J Mol Biol 64*:497–509.

Horovitz A, Fersht AR. 1990. Strategy for analysing the co-operativity of intramolecular interactions in peptides and proteins. *J Mol Biol 214*: 613–617.

Horovitz A, Serrano L, Avron B, Bycroft M, Fersht AR. 1990. Strength and co-operativity of contributions of surface salt bridges to protein stability. *J Mol Biol 216*:1031–1044.

Jordan SR, Pabo CO. 1988. Structure of the lambda complex at 2.5 Å resolution: Details of the repressor–operator interactions. *Science 242*: 893–899.

Lim WA, Sauer RT. 1989. Alternative packing arrangements in the hydrophobic core of lambda repressor. *Nature 339*:31–36.

Lim WA, Sauer RT. 1991. The role of internal packing interactions in determining the structure and stability of a protein. *J Mol Biol 219*:359–376.

Marqusee S, Baldwin RL. 1987. Helix stabilization by $Glu^- \cdots Lys^+$ salt bridges in short peptides of de novo design. *Proc Natl Acad Sci USA 84*:8898–8902.

Marqusee S, Robbins VM, Baldwin RL. 1989. Unusually stable helix formation in short alanine-based peptides. *Proc Natl Acad Sci USA 86*: 5286–5290.

McGregor MJ, Islam SA, Sternberg MJ. 1987. Analysis of the relationship between side-chain conformation and secondary structure in globular proteins. *J Mol Biol 198*:295–310.

Munoz V, Serrano L. 1994. Elucidating the folding problem of helical peptides using empirical parameters. *Nature Struct Biol 1*:399–409.

O'Neil KT, DeGrado WF. 1990. A thermodynamic scale for the helix-forming tendencies of the commonly occurring amino acids [erratum appears in *Science 253*:952, 1991]. *Science 250*:646–651.

Pabo CO, Lewis M. 1982. The operator-binding domain of lambda repressor: Structure and DNA recognition. *Nature 298*:443–447.

Pace CN. 1986. Determination and analysis of urea and guanidine hydrochloride denaturation curves. *Methods Enzymol 131*:266–280.

Reidhaar-Olson J, Parsell DA, Sauer RT. 1990. An essential proline in lambda repressor is required for resistance to intracellular proteolysis. *Biochemistry 29*:7563–7571.

Reidhaar-Olson J, Sauer RT. 1990. Functionally acceptable substitutions in two alpha-helical regions of lambda repressor. *Proteins Struct Funct Genet 7*:306–316.

Santoro MM, Bolen DW. 1988. Unfolding free energy changes determined by the linear extrapolation method. 1. Unfolding of phenylmethanesulfonyl alpha-chymotrypsin using different denaturants. *Biochemistry 27*: 8063–8068.

Scholtz JM, Baldwin RL. 1992. The mechanism of alpha-helix formation by peptides. *Annu Rev Biophys Biomol Struct 21*:95–118.

Serrano L, Fersht AR. 1989. Capping and alpha-helix stability. *Nature 342*:296–299.

Serrano L, Horovitz A, Avron B, Bycroft M, Fersht AR. 1990. Estimating the contribution of engineered surface electrostatic interactions to protein stability by using double-mutant cycles. *Biochemistry 29*:9343–9352.

Stewart JM, Young JD. 1984. *Solid phase peptide synthesis*. Rockford, Illinois: Pierce Chemical Company.

Sueki M, Lee S, Powers SP, Denton JB, Konishi Y, Scheraga HA. 1984. Helix–coil stability constants for the naturally occurring amino acids in water. *Macromolecules 17*:148–155.

Weiss MA, Karplus M, Sauer RT. 1987a. ^{1}H-NMR aromatic spectrum of the operator binding domain of the lambda repressor: Resonance assignment with application to structure and dynamics. *Biochemistry 26*: 890–897.

Weiss MA, Pabo CO, Karplus M, Sauer RT. 1987b. Dimerization of the operator binding domain of phage lambda repressor. *Biochemistry 26*: 897–904.

Wüthrich K. 1986. *NMR of proteins and nucleic acids*. New York: John Wiley & Sons.

Yang A, Honig B. 1992. Electrostatic effects on protein stability. *Curr Opin Struct Biol 2*:40–45.